## **Ensuring Fair Assessment of Solid State Nanopore Sensors with Baseline Current Reporting**

Ming Dong<sup>1</sup>, Zifan Tang<sup>1</sup> and Weihua Guan<sup>1, 2\*</sup>

<sup>1</sup>Department of Electrical Engineering, Pennsylvania State University, University Park, Pennsylvania 16802, United States

<sup>2</sup>Department of Biomedical Engineering, Pennsylvania State University, University Park, Pennsylvania 16802, United States

\* Correspondence should be addressed to wzg111@psu.edu

## **ABSTRACT**

In developing solid-state nanopore sensors for single molecule detection, comprehensive evaluation of the nanopore quality is important. Existing studies typically rely on comparing the noise root mean square (RMS) or power spectrum density (PSD) values. Nanopores exhibiting lower noise values are generally considered superior. This evaluation is valid when the single molecule signal remains consistent. However, the signal can vary, as it is strongly related to the solid-state nanopore size, which is hard to control during fabrication consistently. This work emphasized the need to report the baseline current for evaluating solid-state nanopore sensors. The baseline current offers insight into several experimental conditions, particularly the nanopore size. Our experiments show that a nanopore sensor with more noise is not necessarily worse when considering the signal-to-noise ratio (SNR), particularly when the pore size is smaller. Our findings suggest that relying only on noise comparisons can lead to inaccurate evaluations of solid-state nanopore sensors, considering the inherent variability in fabrication and testing setups among labs and measurements. We propose future studies should include reporting baseline current and sensing conditions. Additionally, using SNR as a primary evaluation tool for nanopore sensors could provide a more comprehensive understanding of their performance.

## Keyword

Solid-state nanopore, performance evaluation, baseline current, noise, signal-to-noise ratio

Solid-state nanopores offer substantial potential in single molecule detection. Despite this promise, their quality evaluation, once fabricated, remains inadequately defined <sup>1-9</sup>. Conventionally, evaluation methodologies involve comparing noise characteristics, specifically the RMS and the PSD <sup>10</sup>. A solid-state nanopore with lower RMS noise and smaller PSD values is generally considered superior. However, this isolated consideration of noise overlooks an essential factor: the nanopore's ability to capture analyte signals. The effectiveness of molecular sensing relies on the SNR, which compares the strength of the signal from translocating molecules to the background noise. Numerous factors can influence a nanopore's noise and signal, such as the analyte size, the nanopore size, salt concentration, pH, and voltage bias <sup>11-18</sup>. Among these parameters, nanopore size presents a significant variable from experiment to experiment. Despite advancements in fabrication techniques, achieving precise nanoscale dimensions and replicating these sizes remains challenging <sup>1,8-9,19</sup>. As such, variations in the single molecule signals generated by these solid-state sensors are anticipated.

For an equitable assessment of fabricated nanopore sensors, it's essential to compare their SNR, which necessitates the knowledge of noise and the signal. It is also crucial to consider the nanopore size, given its exponential impact on signal strength <sup>13, 20-21</sup>. Although the size of solid-state nanopores can be analyzed using transmission electron microscopy (TEM) or scanning electron microscopy (SEM) <sup>4, 6, 9</sup>, these methods are time-consuming and often impractical for routine usage. A more pragmatic approach to determining a nanopore's size involves measuring the *in-situ* baseline current and utilizing physical models <sup>21</sup>. This method offers valuable insights into the nanopore size and testing conditions, such as salt concentration, pH, and voltage bias. These factors are intrinsically connected to the baseline current value, providing a composite overview of these conditions. Unfortunately, the baseline currents of solid-state nanopore sensors are often normalized or zero-ed in research reports <sup>10, 22-23</sup>. This practice of 'zero-ing' the baseline current renders it an unobservable metric, consequently hindering the nanopore size estimation.

In this work, we studied variables influencing the SNR of nanopore sensors. Our findings highlight the crucial need to consider baseline current as part of the evaluation process for solid-state nanopore sensors. We demonstrate through our experiments that a nanopore sensor with a higher noise level isn't necessarily inferior, especially when a smaller pore size is involved. Our research underlines that the sole reliance on noise comparisons could lead to inaccurate assessments of solid-state nanopore sensors, given the inherent discrepancies in fabrication

procedures and measurement setups across different laboratories. Consequently, we strongly advocate that future research incorporate reporting baseline current and sensing conditions as part of their methodology.

For the practical application of solid-state nanopore sensors, the SNR should be the only criterion for determining the nanopore quality as it offers a fair evaluation of signal strength relative to noise. The SNR for a nanopore sensor is defined as:

$$SNR = \frac{\Delta I}{I_{RMS}} \tag{1}$$

where  $I_{RMS}$  is the RMS noise, and  $\Delta I$  is the blockage current induced by the translocation of the molecule.

From the noise perspective, it can be evaluated from either the time or frequency domains. In the time domain, the RMS noise can be calculated as,

$$I_{RMS} = \sqrt{\frac{\sum_{i}^{n} (I_i - I_{Base})}{n}} \tag{2}$$

where  $I_{Base}$  represents the baseline current value (*i.e.*, the mean current of an open nanopore), and n is the number of acquired data points. In the frequency domain, the noise PSD can be calculated as,  $S(f) = 1/2T \lim_{T \to \infty} \left| \int_{-T}^{T} (I_i - I_{Base}) e^{-2\pi i f t} dt \right|^2$ , where f is the bandwidth. It is widely accepted that the noise PSD can be decomposed into four components: 1/f noise, white noise, dielectric noise, and amplifier noise  $^{24-25}$ .

From the signal perspective, the nanopore conductance could be modeled as  $^{21}$ ,  $G = \sigma/(4h/\pi d_{pore}^2 + 1/d_{pore})$ , where G,  $\sigma$ , h, and  $d_{pore}$  represent the nanopore conductance, electrolyte conductivity, membrane thickness, and nanopore diameter, respectively. While this mode is developed for membrane-based nanopores, it can also be generalized to other solid-state nanopores, such as glass nanopores, by adding base and tip diameters of nanopores  $^{26}$ . When analyte translocating in the nanopore, the effective diameter of the nanopore will be,  $d_e = \sqrt{d_{pore}^2 - d_{analyte}^2}$ , where  $d_{analyte}$  is the diameter of the analyte. As a result, the blockage current (i.e., signal strength) could be calculated as,

$$\Delta I = V \times \left[ \sigma \left( \frac{4h}{\pi d_{pore}^2} + \frac{1}{d_{pore}} \right)^{-1} - \sigma \left( \frac{4h}{\pi d_e^2} + \frac{1}{d_e} \right)^{-1} \right]$$
 (3)

A range of variables could impact the noise and the signal (Figure 1a). These variables could include the size of the analyte and the nanopore, the buffer constituents and concentration, the

solution's pH level, and the voltage applied across the nanopore <sup>11-18</sup>. These variables could differ from experiment to experiment, lab to lab, and impact the signal and the noise differently (**Figure 1b**).

Impact of analyte size. Molecules of differing sizes will induce variable effective diameters, which subsequently influence the blockage current, as defined by Eq. 3. The size-dependent nature of the blockage current is due to larger molecules, by occupying more volume of the nanopore, restrict the flow of ions more than smaller molecules, leading to a more significant decrease in ionic current during their translocation. This principle is notably demonstrated in comparing double-stranded DNA (dsDNA) and single-stranded DNA (ssDNA) signals. Due to its larger diameter, dsDNA has a higher blockage current than ssDNA, as evidenced by previous research <sup>12, 18</sup>. Impact of nanopore size. The increase in nanopore size could result in an exponential decrease in the signal strength, as theoretically proposed by Eq. 3<sup>21</sup>. Previous studies showed that white noise and flicker noise are predominant contributors to nanopore noise, and their amplitude is proportional to the nanopore current <sup>25, 27-28</sup>. Consequently, larger diameter nanopores tend to exhibit higher conductance, ionic current, and RMS noise. This results in a potentially diminished SNR, attributable to lower signal strength and elevated noise levels <sup>15</sup>. Unfortunately, the nanopore size presents a control challenge due to the size variation in the fabricated nanopores (Figure 1c&d) 2-6, 8-9, 19, 29-30. Impact of salt concentration. Previous research has investigated the correlation between the concentration of salt and SNR, using SiN<sub>x</sub> nanopore as a representative example <sup>13-15</sup>. The nanopore conductance change could be affected by the translocation of DNA molecules in two ways: First, it decreases due to DNA occupying pore volume and reducing the available charge carriers. Second, the DNA introduces a cloud of mobile counterions, thereby increasing the available charge carriers and positively contributing to the ionic current <sup>13-14</sup>. It was observed that the SNR initially decreases to zero when  $C_{KCl}$  decreases to 0.4 M, subsequently rises to a local maximum at  $C_{KCl} = 0.001$  M, and then decreases at lower concentrations due to increased access resistance <sup>15</sup>. In general, higher concentrations of salt ( $C_{KCl} > 1$  M) are generally preferred for enhanced SNR. Impact of pH. Previous studies suggest that the SiN<sub>x</sub> surface contains two types of surface groups, namely silanol groups and secondary amine groups. 17 These groups could generate either a negatively or positively charged pore wall through dissociation or association reaction with surface protons <sup>31</sup>. Consequently, the pH of the solution could modulate surface charge properties <sup>16-17</sup>. As the surface charge densities vary at different pH values, the number of charge carriers in the nanopore fluctuates accordingly <sup>28</sup>. Based on the data in previous studies <sup>28</sup>, the RMS noise exhibits a maximum value, and the blockage current exhibits a minimum value around pH 6, which might correspond to the point of zero charges in the SiN<sub>x</sub>. Furthermore, it was observed that the SNR is higher in an alkaline environment compared to an acidic environment. Impact of sensing voltage. The bias of sensing voltage across the nanopore is another critical factor in nanopore sensing. Higher sensing voltage leads to a higher baseline current for the nanopore, which induces a higher noise level. Simultaneously, higher sensing voltage generates a higher signal strength, as indicated by Eq. 3. Previous studies demonstrate that the noise level linearly increases with voltage bias, similar to the blockage current <sup>32</sup>. As a result, the SNR of the nanopore is not significantly affected by the sensing voltage. While the event rate could linearly increase with sensing voltage, a high sensing voltage could also risk enlarging the nanopore during measurement <sup>33-34</sup>.

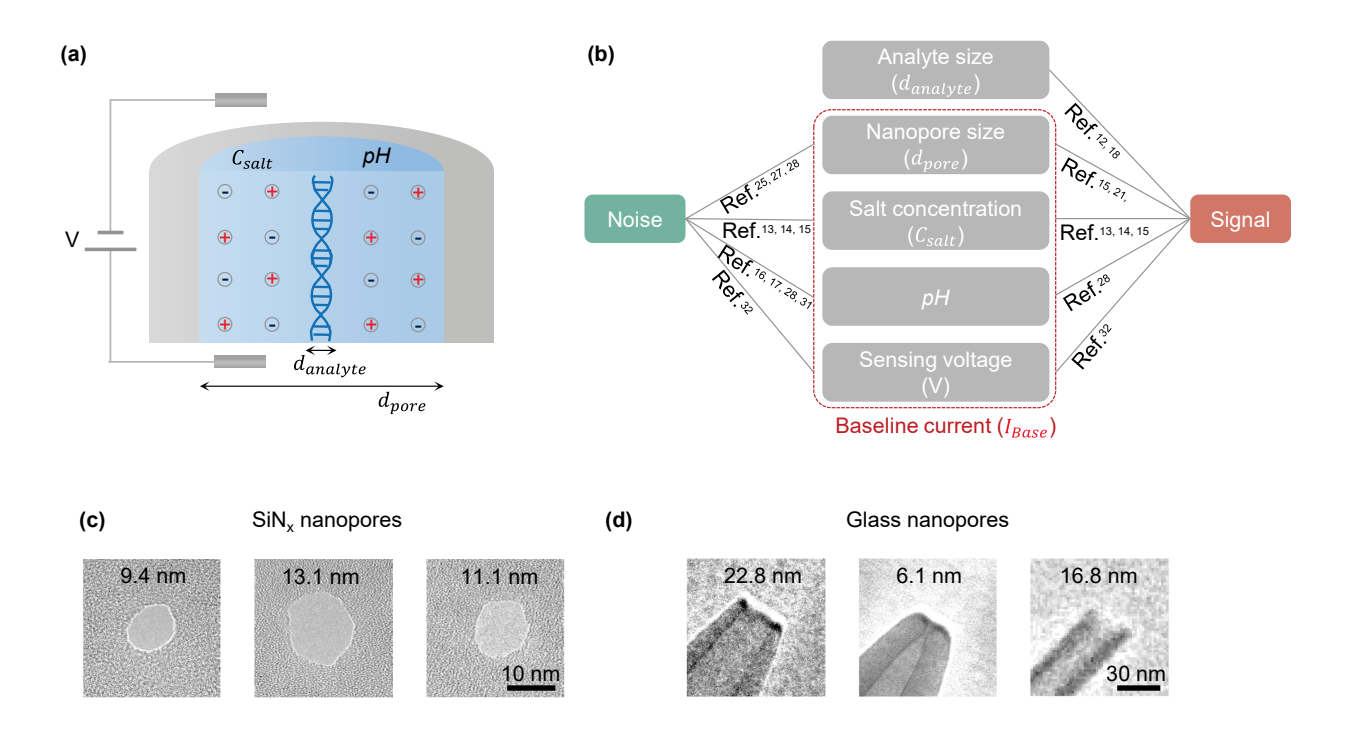


Figure 1. (a) The schematic of nanopore sensing.  $d_{pore}$  is diameter of the nanopore,  $d_{analyte}$  is the diameter of the analyte,  $C_{salt}$  is the concentration of salt,  $\sigma$  is the surface charge density, V is the voltage applied across the nanopore. (b) The factors affecting the noise and signal in solid-state nanopore.  $I_{Base}$  is the nanopore's baseline current. (c) TEM images of SiN<sub>x</sub> nanopores. The nanopores are drilled by TEM. (d) SEM images of glass nanopores.

The factors mentioned above, capable of modulating noise and signal in nanopore sensors,

influence the SNR. However, the heterogeneity of variables across different experiments and labs could create a divergence in nanopore sensor performance assessment. While control over fabrication parameters, solution conditions, and sensing voltage can be made, achieving precision in nanopore size control remains challenging. Despite the established inverse exponential relationship between signal strength and nanopore size, the noise level in solid-state nanopores is less predictable, subject to many factors. Thus, the noise alone could not infer the SNR of nanopore sensors, underscoring the necessity to consider the signal strength.

Although SNR is broadly acknowledged as a reasonable assessment of nanopore quality, the traditional evaluation approach compares noise levels with zero-ed current traces <sup>10, 22-23, 25, 28</sup>. A solid-state nanopore with lower RMS noise and smaller PSD values is generally regarded as superior <sup>10, 15, 22-23, 25</sup>. However, this isolated consideration of noise overlooks an essential factor in SNR: the signal. As shown in Eq. 3, the signal could strongly depend on the size. A smaller nanopore may exhibit higher noise levels, but at the same time, it could also generate a stronger signal. Indeed, we did find this phenomenon in the experiment. To compare the noise performance of nanopores, we initially level the current traces of two fabricated SiN<sub>x</sub> nanopores to zero, as depicted in Figure 2a. Pores #1 and #4 exhibited 26.8 and 20.4 pA RMS noise levels, respectively. Traditional standards would favor pore #4 due to its lower noise level. Yet, upon signal strength assessment in Figure 2b, pore #1 demonstrated a superior signal strength of 2543.8 pA, compared to pore #4's 853.4 pA. As a result, pore #1 has a superior SNR, contradicting the assessment based solely on noise comparison. The baseline current (at 0.3 V) of the two nanopores reveals that the size of pore #1 is smaller than that of pore #4, thereby accounting for the higher SNR. Our findings suggest that a nanopore sensor exhibiting a higher noise level is not necessarily inferior, especially when the pore size is smaller, and could yield a higher SNR.

An inherent limitation of the sole noise comparison is that when current traces get zero-ed, it eradicates information on the nanopore's baseline current, which could indicate the size of the nanopore, a critical factor in determining signal strength. As suggested by **Eq. 3**, the signal strength decreases exponentially with an increase in nanopore size. While several parameters, such as analyte size, salt concentration, pH, and sensing voltage, can be effectively controlled in nanopore sensing experiments, the size of solid-state nanopores is inherently variable <sup>3-6, 9, 29-30</sup>. The nanopore size could vary in fabrication and could even change in sensing experiments due to factors such as heat-induced enlargement <sup>34</sup>. As such, it is essential to incorporate information on

the nanopore's baseline current level ( $I_{Base} = f(\sigma, pH, d_{pore}, V)$ ) and sensing conditions when reporting the nanopore current trace for benchmarking quality. Such information could facilitate a fair comparison of nanopore performance from different laboratories and experiments, enabling informed decisions that optimize sensing conditions and enhancing the sensitivity and reliability of nanopore-based detection and analysis.

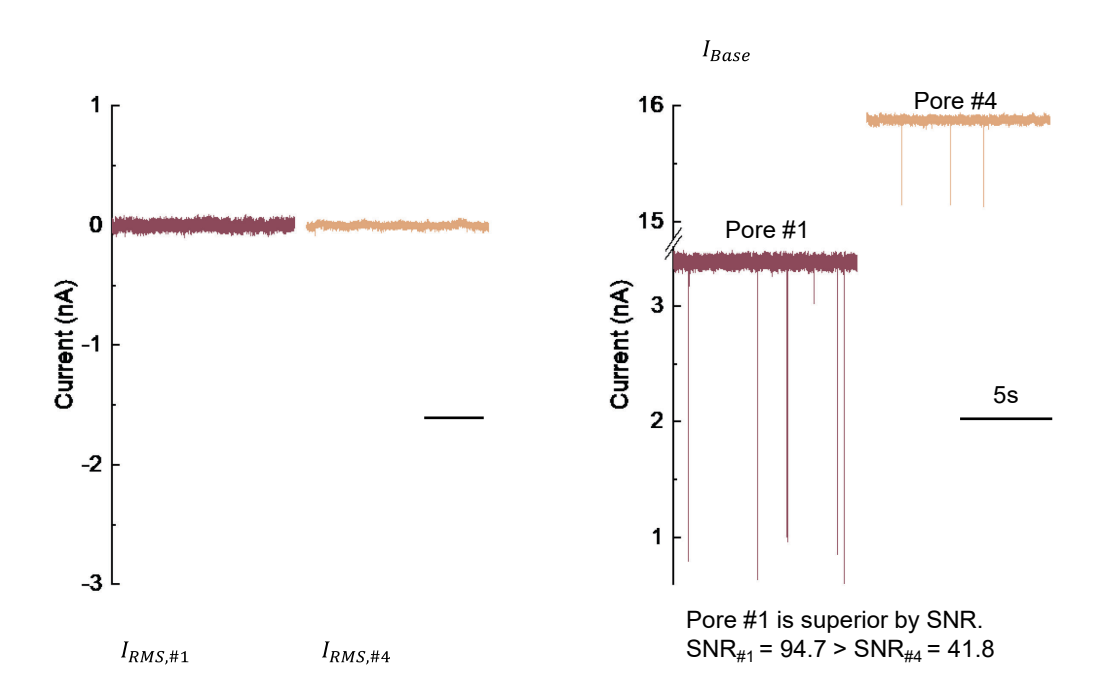


Figure 2. Comparing the performance of 2 CBD  $SiN_x$  nanopores fabricated with the same voltage stress (7 V). (a) Traditional comparison of noise level with zeroed current traces.  $I_{RMS}$  is the noise RMS. (b) Comparison of SNR together with current traces baseline current reported. Traces are obtained by detecting 0.5 nM 20 kbp dsDNA in 2 M LiCl at 0.3 V.

To evaluate the performance of SiN<sub>x</sub> nanopores with varying sizes, we compared the five nanopores fabricated via the CBD method under consistent voltage stress of 7 V. As illustrated in **Figure 3a**, the baseline current of nanopores ranged from 3 nA to 19 nA, signifying the size variation in the fabricated nanopores despite consistent fabrication parameters. **Figure S1** shows the current-voltage (IV) and power spectrum density (PSD) profiles of fabricated nanopores, with no significant PSD variations observed across nanopores of different sizes. We then tested these nanopores using 0.5 nM 20 kbp dsDNA in a 2 M LiCl solution. Upon applying a voltage of 0.3 V across the nanopore, translocation events of the dsDNA were captured, and the dwell time and

amplitude of the blockage current were measured (as depicted in **Figure 3b&c**). Pore #1 shows an extended dwell time which may result from the enhanced interaction between the small nanopore and DNA  $^{20}$ . At the same time, pore #5 also shows an extended dwell time. Although the larger pore interacts less with DNA molecules, the reduced electric field inside the pore leads to slower DNA translocation  $^{35-36}$ . The summarized noise levels of the SiN<sub>x</sub> nanopores (**Figure 3d**) reveal no substantial correlation with the baseline current, suggesting that the noise level in SiN<sub>x</sub> nanopores exhibits a relatively stochastic behavior. However, as depicted in **Figure 3e**, the signal strength demonstrates an exponential decrease with an increase in baseline current. Analysis of the SNR among the five nanopores (**Figure 3f**) illustrates a generally inverse correlation between the SNR and nanopore baseline current. Notably, the random noise level in SiN<sub>x</sub> nanopores means that smaller pores do not consistently yield a higher SNR. The SNR values from pores #2, #3, and #4 exemplify this; even though smaller pores produce increased signal intensities, the stochastic noise behavior results in comparable SNR across these pores. Further, our previous comparative analysis of pore # 1 and pore # 4 evidenced that a lower RMS noise in a nanopore does not guarantee a higher signal strength and SNR.

Additionally, we evaluated glass nanopores to ascertain the influence of their size on RMS noise, signal strength, and SNR. The resultant findings are compiled in Figure 4. Although no significant extended dwell time was observed in the smallest pore #1, it was observed in larger pores, such as pores #6 and #7 (Figure 4b). This extended dwell time can be attributed to slower translocation caused by a smaller electric field in these larger pores <sup>36</sup>. In addition, the PSD profiles in Figure S1 demonstrate that the noise intensity for glass nanopores is approximately two orders of magnitude lower across all frequencies relative to SiN<sub>x</sub> nanopores. This variation could be attributed to differing dielectric loss constants, which are smaller for quartz glass (2×10<sup>-4</sup>) as compared to SiN<sub>x</sub> (1.4×10<sup>-3</sup>) <sup>25, 37-38</sup>, resulting in reduced noise levels for glass nanopores. Furthermore, factors such as nanopore wall surface roughness, surface chemistry, and defects could also contribute to varied noise profiles <sup>27, 39</sup>. Besides, a positive correlation was observed between RMS noise and glass nanopore baseline current, as presented in Figure 4d. This trend between nanopore size and RMS noise levels is more pronounced in glass nanopores compared to SiN<sub>x</sub> CBD nanopores. While the underlying mechanisms remain to be fully explored, the observed variability in noise trend across SiN<sub>x</sub> nanopores could be attributed to several factors. Variations in parameters such as surface charge density, pore geometry, and membrane defect density may

introduce stochastic fluctuations in ionic current, thereby contributing to inconsistent noise profiles in SiN<sub>x</sub> nanopores of different sizes <sup>15, 25, 27-28</sup>. As the glass nanopore was used for dsDNA detection, the blockage current amplitude exhibited an exponential decrease with the nanopore size increment (**Figure 4e**), consistent with **Eq. 3**. Overall, the SNR of the glass nanopore also displayed a negative correlation with the nanopore baseline current, as shown in **Figure 4f**. These correlations suggest that smaller glass nanopores provide a higher SNR than larger ones, predominantly due to reduced RMS noise levels and enhanced signal intensity.

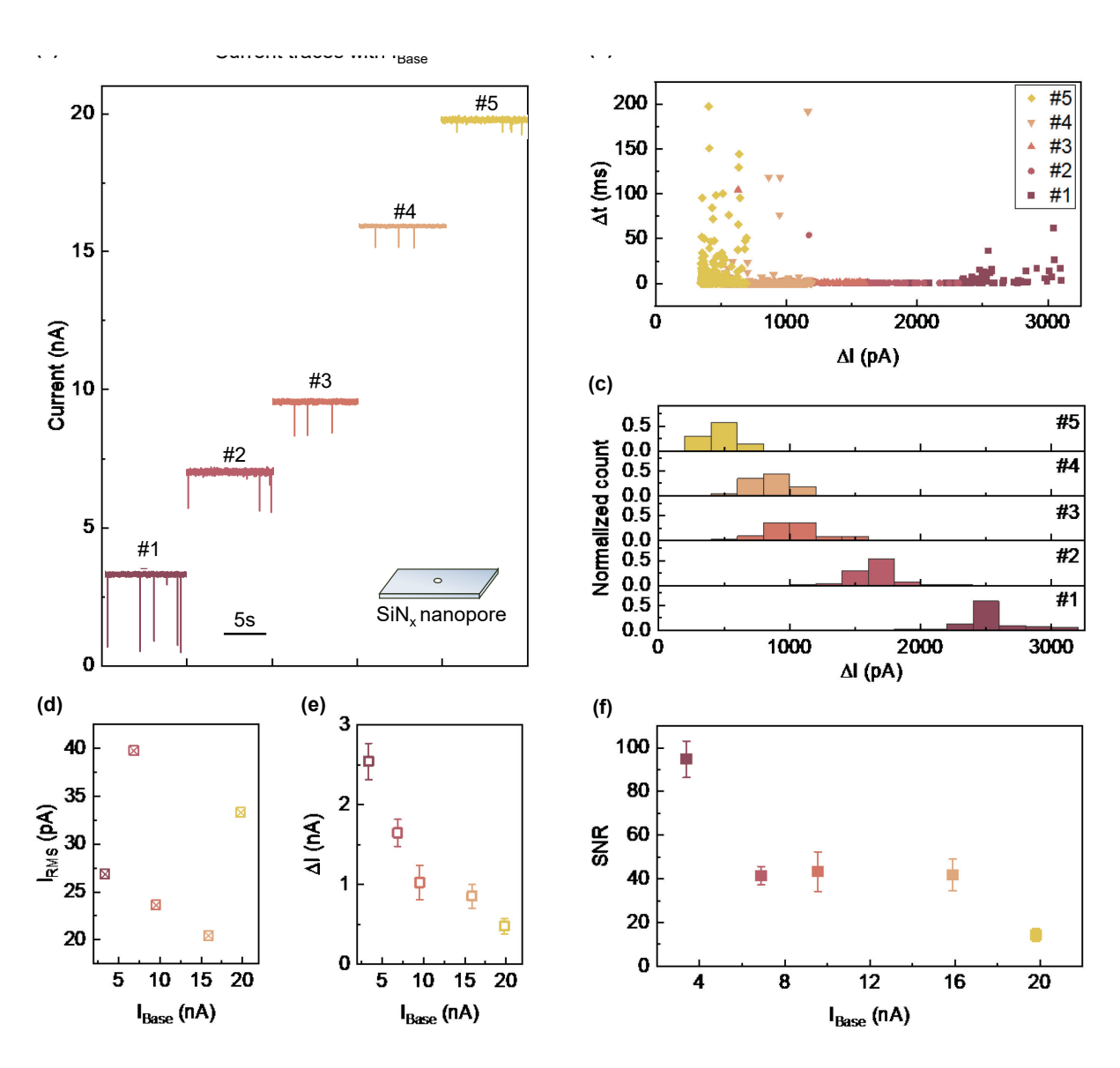


Figure 3. Comparing the performance of  $5 \, \mathrm{SiN_x}$  nanopores fabricated with the same voltage stress (7 V). (a) Current traces obtained through detection of 0.5 nM 20 kbp dsDNA in 2 M LiCl at 0.3 V. (b) Scatter plot of dwell time and blockage current. (c) Histograms of blockage current ( $\Delta I$ ,

signal strength) obtained from 7 nanopores. Pore #1 has 192 events, #2 has 224 events, #3 has 239 events, #4 has 955 events, and #5 has 318 events. Correlation between nanopore's baseline current and RMS noise (c), signal (d), and SNR (e).

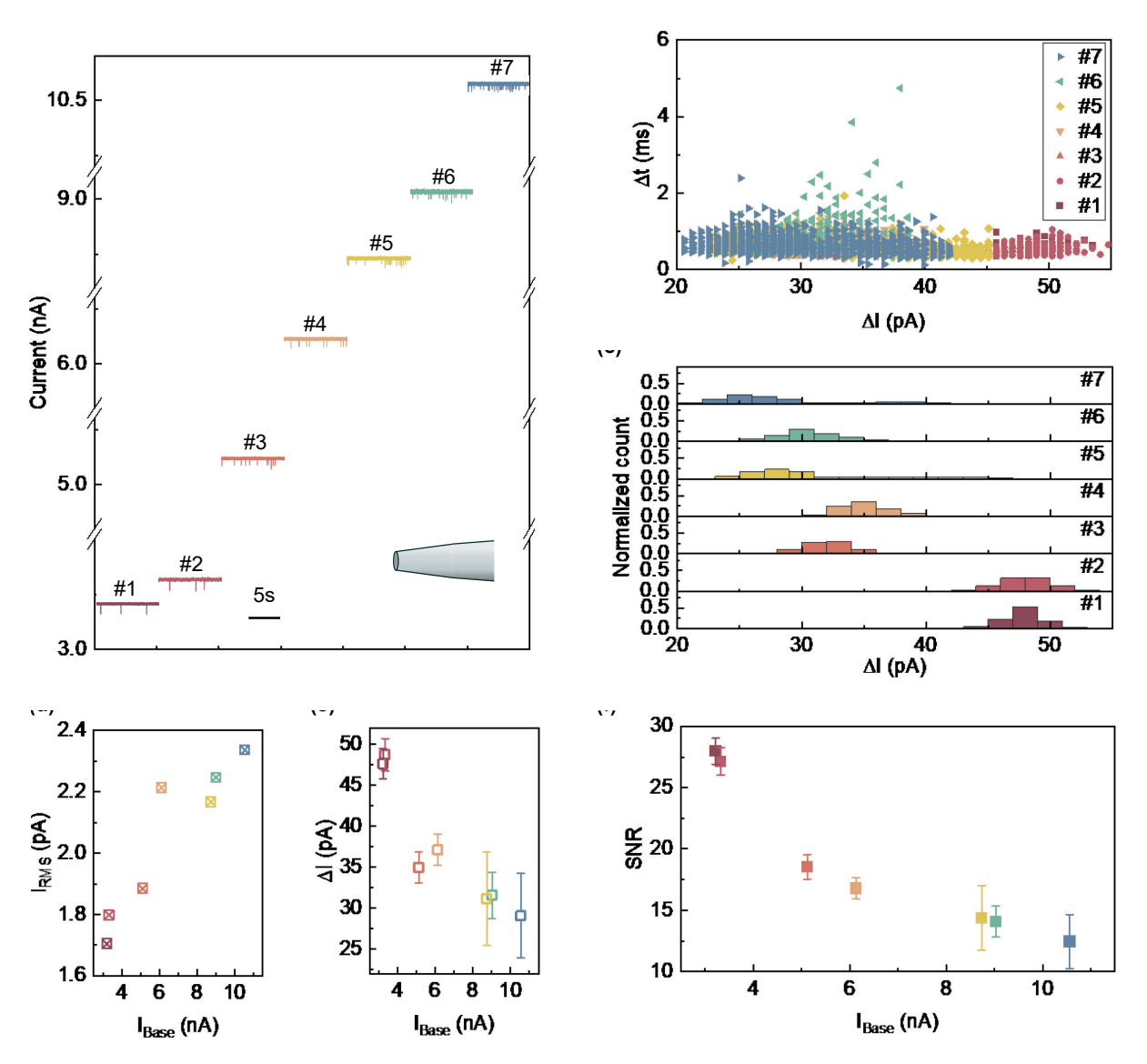


Figure 4. Comparing the performance of 7 glass nanopores fabricated with the same parameters. (a) Current traces obtained through detection of 4 nM 2 kbp dsDNA in 2 M LiCl at 0.3 V. (b) Scatter plot of dwell time and blockage current. (c) Histograms of blockage current (Δ*I*, signal strength) obtained from 7 nanopores. Pore #1 has 251 events, #2 has 266 events, #3 has 731 events, #4 has 445 events, #5 has 1138 events, #6 has 592 events, and #7 has 1475 events. Correlation between nanopore's baseline current and RMS noise (c), signal (d), and SNR (e).

In conclusion, the variability in nanopore size stemming from solid-state nanopore fabrication processes and testing protocols inherently causes fluctuations in single molecule signals <sup>2-6, 8-9, 19,</sup>

<sup>29-30</sup>. The result is that noise RMS or PSD comparison alone could provide misleading quality assessment across different experiments due to a lack of consideration for single-molecule signals. Our experiments demonstrated that higher noise levels in solid-state nanopores do not necessarily indicate inferior quality, especially when smaller pore sizes are involved. While our study found that smaller glass pores yield a higher SNR, this trend isn't always true for SiN<sub>x</sub> nanopores due to their stochastic noise behavior. The critical information encapsulated in the baseline current, especially nanopore size, is often disregarded in many studies, rendering this crucial data unobservable. Our findings thus emphasize the significant role of the baseline current in the SNR assessment process for solid-state nanopore sensors. Building on these findings, we propose that integrating baseline current reporting and sensing conditions into study methodologies can enhance benchmarking consistency in future research.

See supplementary material for the experiment details, nanopore fabrication methods, DNA sensing data analysis, and electrical characteristics of SiN<sub>x</sub> and glass nanopores.

This work was partially supported by the National Science Foundation under Grant No. NSF2045169. Any opinions, findings, and conclusions or recommendations expressed in this work are those of the authors and do not necessarily reflect the views of the National Science Foundation. The authors have no conflicts to disclose. W.G. conceived the concept and supervised the study. M.D. performed CBD nanopore and glass nanopore experiments. Z. T. helped build the setup. W.G. and M.D. co-wrote the manuscript, discussed it with all the other authors. The data that support the findings of this study are available from the corresponding author upon reasonable request.

## **REFERENCES**

- 1. Chen, C.-H.; Chang, X.; Wu, C.-S., A novel shaped-controlled fabrication of nanopore and its applications in quantum electronics. *Scientific reports* **2019**, *9* (1), 1-7.
- 2. Lanyon, Y. H.; De Marzi, G.; Watson, Y. E.; Quinn, A. J.; Gleeson, J. P.; Redmond, G.; Arrigan, D. W., Fabrication of nanopore array electrodes by focused ion beam milling. *Analytical chemistry* **2007**, *79* (8), 3048-3055.
- 3. Kwok, H.; Briggs, K.; Tabard-Cossa, V., Nanopore fabrication by controlled dielectric breakdown. *Plos One* **2014**, *9* (3), e92880.
- 4. Gilboa, T.; Zrehen, A.; Girsault, A.; Meller, A., Optically-monitored nanopore fabrication using a focused laser beam. *Scientific reports* **2018**, *8* (1), 1-10.

- 5. Yamazaki, H.; Hu, R.; Zhao, Q.; Wanunu, M., Photothermally assisted thinning of silicon nitride membranes for ultrathin asymmetric nanopores. *ACS Nano* **2018**, *12* (12), 12472-12481.
- 6. Ying, C.; Houghtaling, J.; Eggenberger, O. M.; Guha, A.; Nirmalraj, P.; Awasthi, S.; Tian, J.; Mayer, M., Formation of Single Nanopores with Diameters of 20–50 nm in Silicon Nitride Membranes Using Laser-Assisted Controlled Breakdown. *ACS Nano* **2018**, *12* (11), 11458-11470.
- 7. Waugh, M.; Briggs, K.; Gunn, D.; Gibeault, M.; King, S.; Ingram, Q.; Jimenez, A. M.; Berryman, S.; Lomovtsev, D.; Andrzejewski, L., Solid-state nanopore fabrication by automated controlled breakdown. *Nature Protocols* **2020**, *15* (1), 122-143.
- 8. Yemini, M.; Hadad, B.; Liebes, Y.; Goldner, A.; Ashkenasy, N., The controlled fabrication of nanopores by focused electron-beam-induced etching. *Nanotechnology* **2009**, *20* (24), 245302.
- 9. Yanagi, I.; Akahori, R.; Hatano, T.; Takeda, K.-i., Fabricating nanopores with diameters of sub-1 nm to 3 nm using multilevel pulse-voltage injection. *Scientific reports* **2014**, *4* (1), 1-7.
- 10. Tabard-Cossa, V.; Trivedi, D.; Wiggin, M.; Jetha, N. N.; Marziali, A., Noise analysis and reduction in solid-state nanopores. *Nanotechnology* **2007**, *18* (30), 305505.
- 11. Cressiot, B.; Greive, S. J.; Mojtabavi, M.; Antson, A. A.; Wanunu, M., Thermostable virus portal proteins as reprogrammable adapters for solid-state nanopore sensors. *Nature communications* **2018**, *9* (1), 4652.
- 12. Skinner, G. M.; van den Hout, M.; Broekmans, O.; Dekker, C.; Dekker, N. H., Distinguishing single-and double-stranded nucleic acid molecules using solid-state nanopores. *Nano Letters* **2009**, *9* (8), 2953-2960.
- 13. Chang, H.; Kosari, F.; Andreadakis, G.; Alam, M.; Vasmatzis, G.; Bashir, R., DNA-mediated fluctuations in ionic current through silicon oxide nanopore channels. *Nano letters* **2004**, *4* (8), 1551-1556.
- 14. Smeets, R. M.; Keyser, U. F.; Krapf, D.; Wu, M.-Y.; Dekker, N. H.; Dekker, C., Salt dependence of ion transport and DNA translocation through solid-state nanopores. *Nano letters* **2006**, *6* (1), 89-95.
- 15. Smeets, R. M.; Keyser, U. F.; Dekker, N. H.; Dekker, C., Noise in solid-state nanopores. *Proceedings of the National Academy of Sciences* **2008**, *105* (2), 417-421.
- 16. Sonnefeld, J., Determination of surface charge density parameters of silicon nitride. *Colloids and Surfaces A: Physicochemical and Engineering Aspects* **1996**, *108* (1), 27-31.
- 17. Lin, K.; Li, Z.; Tao, Y.; Li, K.; Yang, H.; Ma, J.; Li, T.; Sha, J.; Chen, Y., Surface charge density inside a silicon nitride nanopore. *Langmuir* **2021**, *37* (35), 10521-10528.
- 18. Thangaraj, V.; Lepoitevin, M.; Smietana, M.; Balanzat, E.; Bechelany, M.; Janot, J.-M.; Vasseur, J.-J.; Subramanian, S.; Balme, S., Detection of short ssDNA and dsDNA by current-voltage measurements using conical nanopores coated with Al 2 O 3 by atomic layer deposition. *Microchimica Acta* **2016**, *183*, 1011-1017.
- 19. Storm, A.; Chen, J.; Ling, X.; Zandbergen, H.; Dekker, C., Fabrication of solid-state nanopores with single-nanometre precision. *Nature materials* **2003**, *2* (8), 537-540.
- 20. Wanunu, M.; Sutin, J.; McNally, B.; Chow, A.; Meller, A., DNA translocation governed by interactions with solid-state nanopores. *Biophysical journal* **2008**, *95* (10), 4716-4725.
- 21. Kowalczyk, S. W.; Grosberg, A. Y.; Rabin, Y.; Dekker, C., Modeling the conductance and DNA blockade of solid-state nanopores. *Nanotechnology* **2011**, *22* (31), 315101.
- 22. Fragasso, A.; Schmid, S.; Dekker, C., Comparing current noise in biological and solid-state nanopores. *ACS nano* **2020**, *14* (2), 1338-1349.
- 23. Lee, M.-H.; Kumar, A.; Park, K.-B.; Cho, S.-Y.; Kim, H.-M.; Lim, M.-C.; Kim, Y.-R.; Kim, K.-B., A low-noise solid-state nanopore platform based on a highly insulating substrate.

- *Scientific reports* **2014,** *4* (1), 1-7.
- 24. Lee, K.; Park, K. B.; Kim, H. J.; Yu, J. S.; Chae, H.; Kim, H. M.; Kim, K. B., Recent progress in solid state nanopores. *Advanced materials* **2018**, *30* (42), 1704680.
- 25. Liang, S.; Xiang, F.; Tang, Z.; Nouri, R.; He, X.; Dong, M.; Guan, W., Noise in nanopore sensors: sources, models, reduction, and benchmarking. *Nanotechnology and Precision Engineering* **2020**, *3* (1), 9-17.
- 26. Makra, I.; Gyurcsányi, R. E., Electrochemical sensing with nanopores: A mini review. *Electrochemistry communications* **2014**, *43*, 55-59.
- 27. Fragasso, A.; Pud, S.; Dekker, C., 1/f noise in solid-state nanopores is governed by access and surface regions. *Nanotechnology* **2019**, *30* (39), 395202.
- 28. Wen, C.; Zeng, S.; Arstila, K.; Sajavaara, T.; Zhu, Y.; Zhang, Z.; Zhang, S.-L., Generalized noise study of solid-state nanopores at low frequencies. *ACS sensors* **2017**, *2* (2), 300-307.
- 29. Roshan, K. A.; Tang, Z.; Guan, W., High fidelity moving Z-score based controlled breakdown fabrication of solid-state nanopore. *Nanotechnology* **2019**, *30* (9), 095502.
- 30. Tang, Z.; Dong, M.; He, X.; Guan, W., On Stochastic Reduction in Laser-Assisted Dielectric Breakdown for Programmable Nanopore Fabrication. *ACS Applied Materials & Interfaces* **2021**, *13* (11), 13383-13391.
- 31. Čerović, L. S.; Milonjić, S. K.; Bahloul-Hourlier, D.; Doucey, B., Surface properties of silicon nitride powders. *Colloids and Surfaces A: Physicochemical and Engineering Aspects* **2002**, 197 (1-3), 147-156.
- 32. Liu, Q.; Wu, H.; Wu, L.; Xie, X.; Kong, J.; Ye, X.; Liu, L., Voltage-driven translocation of DNA through a high throughput conical solid-state nanopore. **2012**.
- 33. Nouri, R.; Tang, Z.; Guan, W., Calibration-free nanopore digital counting of single molecules. *Analytical chemistry* **2019**, *91* (17), 11178-11184.
- 34. Tsutsui, M.; Arima, A.; Yokota, K.; Baba, Y.; Kawai, T., Ionic heat dissipation in solid-state pores. *Science Advances* **2022**, *8* (6), eabl7002.
- 35. Fanget, A. Towards Tunneling Electrodes for Nanopore-Based DNA Sequencing; EPFL: 2013.
- 36. Getpreecharsawas, J.; McGrath, J. L.; Borkholder, D. A., The electric field strength in orifice-like nanopores of ultrathin membranes. *Nanotechnology* **2015**, *26* (4), 045704.
- 37. Lukianova, O.; Sirota, V., Dielectric properties of silicon nitride ceramics produced by free sintering. *Ceramics International* **2017**, *43* (11), 8284-8288.
- 38. De, A.; Rao, K., Dielectric properties of synthetic quartz crystals. *Journal of materials science* **1988**, *23*, 661-664.
- 39. Powell, M. R.; Martens, C.; Siwy, Z. S., Asymmetric properties of ion current 1/f noise in conically shaped nanopores. *Chemical Physics* **2010**, *375* (2-3), 529-535.